LETTERS

A PtdIns4,5P_2-regulated nuclear poly(A) polymerase controls expression of select mRNAs

David L. Mellman[1]*, Michael L. Gonzales[1]*, Chunhua Song[2]*, Christy A. Barlow[2]*, Ping Wang[3], Christina Kendziorski[3] & Richard A. Anderson[1,2]

Phosphoinositides are a family of lipid signalling molecules that regulate many cellular functions in eukaryotes. Phosphatidylinositol-4,5-bisphosphate (PtdIns4,5P_2), the central component in the phosphoinositide signalling circuitry, is generated primarily by type I phosphatidylinositol 4-phosphate 5-kinases (PIPKIα, PIPKIβ and PIPKIγ)[1]. In addition to functions in the cytosol, phosphoinositides are present in the nucleus[2,3], where they modulate several functions[4–6]; however, the mechanism by which they directly regulate nuclear functions remains unknown. PIPKIs regulate cellular functions through interactions with protein partners, often PtdIns4,5P_2 effectors, that target PIPKIs to discrete subcellular compartments, resulting in the spatial and temporal generation of PtdIns4,5P_2 required for the regulation of specific signalling pathways[1,7]. Therefore, to determine roles for nuclear PtdIns4,5P_2 we set out to identify proteins that interacted with the nuclear PIPK, PIPKIα. Here we show that PIPKIα co-localizes at nuclear speckles and interacts with a newly identified non-canonical poly(A) polymerase, which we have termed Star-PAP (nuclear speckle targeted PIPKIα regulated-poly(A) polymerase) and that the activity of Star-PAP can be specifically regulated by PtdIns4,5P_2. Star-PAP and PIPKIα function together in a complex to control the expression of select mRNAs, including the transcript encoding the key cytoprotective enzyme haem oxygenase-1 (refs 8, 9) and other oxidative stress response genes by regulating the 3′-end formation of their mRNAs. Taken together, the data demonstrate a model by which phosphoinositide signalling works in tandem with complement pathways to regulate the activity of Star-PAP and the subsequent biosynthesis of its target mRNA. The results reveal a mechanism for the integration of nuclear phosphoinositide signals and a method for regulating gene expression.

To identify nuclear PIPKIα-interacting proteins, the nuclear speckle-targeting region of PIPKIα (amino-acid residues 440–562; Fig. 1a) was used as bait in a yeast two-hybrid screen. Among the interactors identified was a protein we have named Star-PAP. Star-PAP is a member of the DNA polymerase β-like superfamily of nucleotidyltransferases and is most closely related to poly(A) polymerases (PAPs). Star-PAP is unique among known PAPs[10,11] (Fig. 1b) in that it contains a split PAP domain linked by a proline-rich region, an amino-terminal C_2H_2 zinc-finger, an RNA recognition motif, a PAP catalytic and core domain, a PAP-associated domain, an R/S repeat and a nuclear localization signal (Fig. 1b). Star-PAP has putative family members throughout species (Supplementary Fig. 2) and is expressed in numerous cultured cell lines and ubiquitously in humans (Supplementary Fig. 3).

The interaction between Star-PAP and PIPKIα was confirmed by an *in vitro* glutathione *S*-transferase (GST) pull-down assay. Star-PAP bound to GST–PIPKIα and the GST–PIPKIα carboxy terminus, but not to GST alone (Fig. 1c). Immunoprecipitation of endogenous Star-PAP resulted in co-immunoprecipitation of PIPKIα (Fig. 1d) but not other PIPKI isoforms (data not shown), showing that this interaction occurs *in vivo*. Star-PAP localizes at nuclear speckles, as shown by its co-localization with PIPKIα and Sm proteins and by its loss at speckles on RNA-mediated interference (RNAi) knockdown (Fig. 1e, f). The targeting of Star-PAP with PIPKIα and PtdIns4,5P_2, to a compartment where pre-mRNA processing factors and phosphoinositide metabolism are concentrated[3,12] suggested that Star-PAP functions in mRNA biosynthesis and may be regulated by phosphoinositides.

On the basis of the sequence homology between Star-PAP and known poly(A) polymerases (Supplementary Fig. 4) Star-PAP was assayed for PAP activity[13]. Recombinant purified Star-PAP extended an A_{15} RNA primer with [α-^{32}P]ATP (Fig. 2a). As with known PAPs, Star-PAP activity was inhibited by the chain terminator cordycepin triphosphate (0–5.0 mM) (Fig. 2b), and nucleotide incorporation into the RNA substrate by Star-PAP was selective for ATP (Fig. 2c). Moreover, 3′ tails generated with all four rNTPs in the reaction mixture were digested with oligo(dT)/RNase H, indicating that the extension of the RNA primer is primarily through the addition of AMP (Fig. 2d). Mutations of catalytic residues (Supplementary Fig. 4, asterisk) within the nucleotidyl transferase motif[14] enfeebled PAP activity (Fig. 2e). Together these data indicate that Star-PAP possesses PAP activity.

Recently, recombinant Star-PAP purified from HeLa cells was reported to have terminal uridylyl transferase (TUTase) activity specific for U6 snRNA *in vitro*[15]. Under both defined TUTase and PAP assay conditions, Star-PAP has the capacity to transfer UMP residues to RNA (Supplementary Fig. 5). However, the concentration of ATP in cells is much greater than that of UTP[16]. We therefore subjected Star-PAP to an *in vitro* nucleotide competition assay to determine its preferred nucleotide substrate. Star-PAP activity towards UTP was effectively inhibited by the addition of excess ATP, but not vice versa (Supplementary Fig. 5). Although Star-PAP does indeed have genuine TUTase activity, these data show that, with *in vivo* ratios of rNTPs, Star-PAP preferentially uses ATP as a nucleotide substrate, indicating that it functions primarily as a poly(A) polymerase.

Because Star-PAP interacts with PIPKIα, we determined whether Star-PAP is an effector of the PIPKIα product PtdIns4,5P_2. In the presence of 50 μM PtdIns4,5P_2, Star-PAP activity was markedly stimulated, particularly with regard to products more than 200 nucleotides in length (Fig. 2f, h, i). Other phosphoinositides did not affect Star-PAP activity, and no phosphoinositide had an effect on PAPα activity (Fig. 2g, h), demonstrating that PtdIns4,5P_2 stimulation is a unique trait of Star-PAP. In addition, inositol-1,4,5-trisphosphate

[1]Program in Molecular and Cellular Pharmacology, [2]Department of Pharmacology, and [3]Department of Biostatistics and Medical Informatics, University of Wisconsin Medical School, University of Wisconsin-Madison, 1300 University Avenue, Madison, Wisconsin 53706, USA.
*These authors contributed equally to this work.

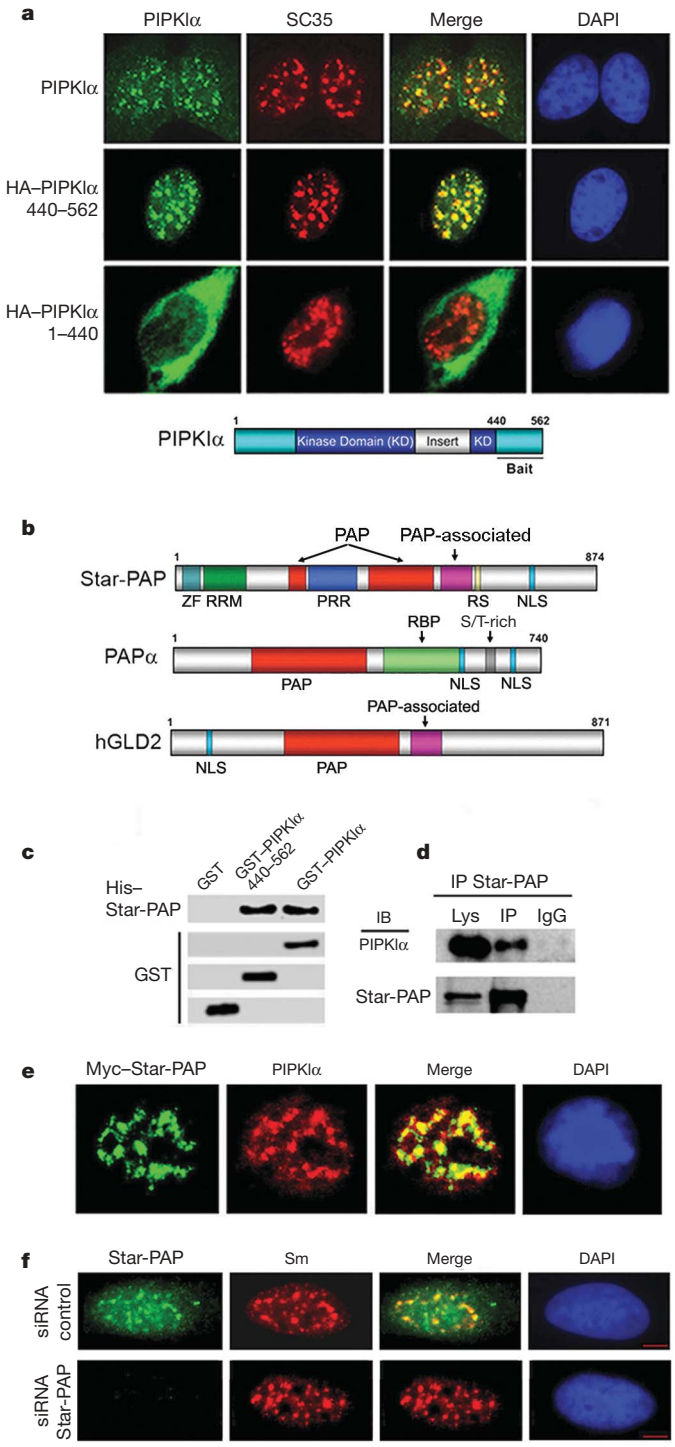

Figure 1 | Identification of a nuclear-localized PIPKIα-interacting protein. **a**, Localization of PIPKIα, haemagglutinin (HA)-tagged PIPKIα C terminus (residues 1–439), HA–PIPKIα N terminus (residues 440–562) (green), SC-35 (red) and 4′,6-diamidino-2-phenylindole (blue) in HeLa cells. The underlined region of the PIPKIα diagram represents bait used in the yeast two-hybrid screen. **b**, Diagram of Star-PAP domain arrangement compared with those of PAPα and human Germ line development 2 (hGld2). NLS, nuclear localization signal; PRR, proline-rich region; RBD, RNA-binding domain; RRM, RNA recognition motif; RS, arginine/serine repeat; ZF, zinc-finger. **c**, *In vitro* GST pull-down with His–Star-PAP and GST–PIPKIα full-length and C terminus. **d**, Immunoprecipitation (IP) of Star-PAP and detection of associated PIPKIα. IB, immunoblot. **e**, Subnuclear localization of Myc-tagged Star-PAP (green) and endogenous PIPKIα (red). **f**, Subnuclear localization of endogenous Star-PAP (green) and Sm (red) after RNAi knockdown with control oligonucleotide (top) or oligonucleotide specific for Star-PAP (bottom). Scale bar, 5 μm.

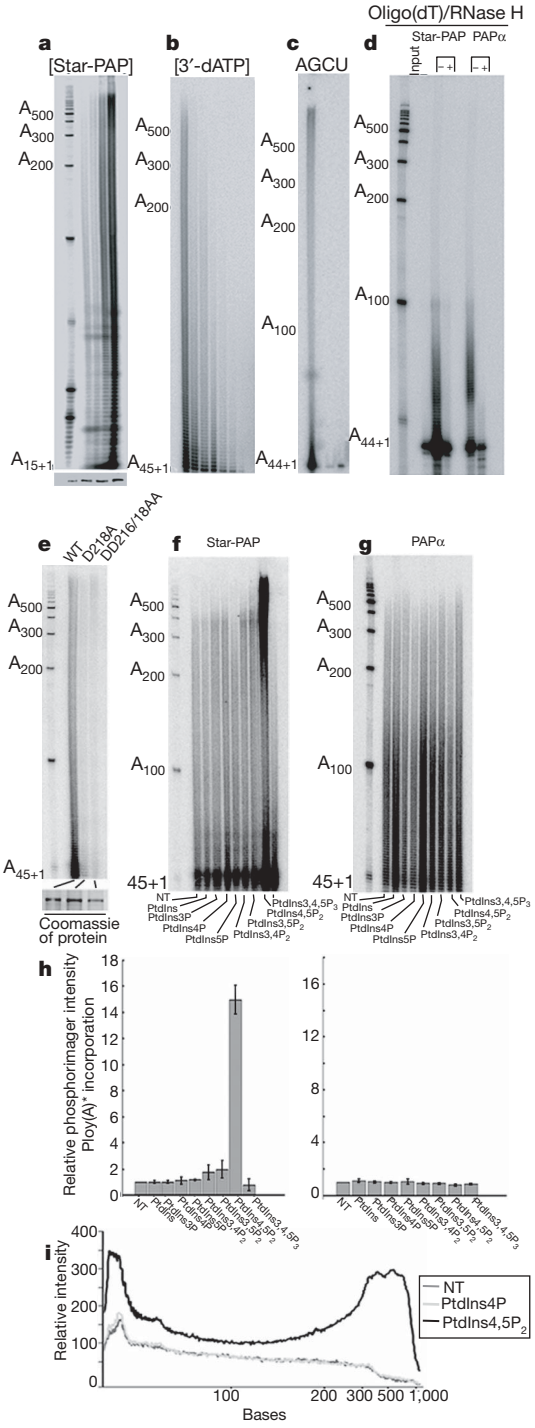

Figure 2 | Star-PAP has poly(A) polymerase activity that is stimulated by PtdIns4,5P$_2$. **a**, The activity of His-Star-PAP (0–1.25 μM) towards A_{15} RNA primer. Anti-T7 western blot (bottom) demonstrates protein levels. **b**, Effects of cordycepin triphosphate on His–Star-PAP activity. **c**, Star-PAP activity towards all four rNTPs. **d**, Oligo(dT)/RNase H treatment of Star-PAP-generated RNA product. **e**, Effects on mutations of conserved catalytic residues in Star-PAP. Coomassie blue stain demonstrates protein levels. **f**, **g**, Effects of 50 μM inositol phospholipid micelles on His–Star-PAP (**f**) and PAPα (1 μM) (**g**) activity. NT, non-treated vehicle-only control. **h**, Incorporation of [α-^{32}P]ATP into poly(A)$^+$ products larger than A_{200} in the presence of phosphoinositide micelles by Star-PAP and PAPα from **f** and **g** ($n = 3$). Error bars represent s.e.m. **i**, Relative distributions of poly(A)$^+$ products from non-treated (NT), PtdIns4P-treated and PtdIns4,5P$_2$-treated Star-PAP from **f**.

did not stimulate Star-PAP activity, demonstrating that this regulation is specific for the lipid species (data not shown).

PAPs associate with protein partners that define their function *in vivo*[11,17–19]. Canonical PAPα associates *in vivo* with factors required for the polyadenylation of mRNA, including cleavage and polyadenylation specificity factor (CPSF) and cleavage stimulation factor (CstF) subunits, symplekin and RNA polymerase II (RNA Pol II)[10,18,20–22]. Similarly, endogenous Star-PAP co-immunoprecipitated with CPSF-73, RNA Pol II and symplekin (Fig. 3a, b). Endogenous PIPKIα specifically associated with Flag-tagged Star-PAP and was able to generate PtdIns4,5P_2 *in vitro* (Fig. 3c), which suggests that in accordance with the model of spatial phosphoinositide generation defining its function, the production of PtdIns4,5P_2 *de novo* occurs in proximity to Star-PAP to regulate its activity *in vivo*. To compare their associated protein complexes, Flag–Star-PAP and Flag–PAPα were expressed and affinity purified in parallel from HEK-293 cells. Both Star-PAP and PAPα associated with mRNA 3′-processing factors (Supplementary Fig. 6). PAPα was not detected in the Star-PAP complex; nor was the reverse true (Fig. 4g and Supplementary Fig. S6); in addition, the exosome components Rrp6 and Rrp46 (ref. 17) were not detected in the Star-PAP complex (data not shown), indicating specificity with pre-mRNA 3′-processing factors. Phylogenetic analysis demonstrates that Star-PAP clusters with PAPs that polyadenylate mRNAs (Supplementary Fig. 7), supporting the hypothesis that Star-PAP functions as a PAP in the 3′-end formation of mRNAs.

Polyadenylation of mRNA is critical for its stability[23,24]. Therefore, a loss of Star-PAP would be predicted to decrease the level of mRNAs that it polyadenylates. Moreover, if PIPKIα has a functional relationship with Star-PAP, knockdown of PIPKIα should cause a decrease in a pool of target mRNAs that require both Star-PAP and PIPKIα for their maturation. To test this, we knocked down Star-PAP or PIPKIα and performed a microarray analysis of total polyadenylated mRNAs from each group. A significant (conditional false discovery rate ≤ 0.01) change in transcript level compared with control cells ($n = 3$) was detected for 4,481 genes with *Star-PAP* RNAi knockdown and 4,542 genes with *PIPKIα* RNAi knockdown. There was an overlap of 2,350 significant gene changes in both conditions, of which 2,262 were in the same direction (Fig. 3d).

A large group of the identified genes encode proteins involved in detoxification and/or oxidative stress response. Some of these, including those encoding haem oxygenase-1 (*HO-1*), NAD(P)H:quinone oxidoreductase 1 (*NQO1*), apolipoprotein E (*APOE*), peroxiredoxin 1 (*PRDX1*), glutathione *S*-transferase κ1 (*GSTK1*) and aldehyde dehydrogenase 2 family (mitochondrial) (*ALDH2*), were chosen for validation by quantitative real-time RT–PCR (qRT–PCR). The expression levels of these candidate mRNAs were consistent with the microarray analysis, demonstrating that Star-PAP is required for the expression of these mRNAs. *PIPKIα* RNAi knockdown also significantly decreased the expression levels of these same mRNAs, indicating that PIPKIα modulates select Star-PAP-dependent gene expression (Fig. 3e). Knockdown of both Star-PAP and PIPKIα showed no additive effect on the loss of *HO-1* or *NQO1* mRNA, providing evidence that Star-PAP and PIPKIα function in a common pathway to control their expression (data not shown).

To determine direct targets of Star-PAP, RNA immunoprecipitation[25] was used. Star-PAP was associated with *HO-1* mRNA but not with the non-target mRNAs encoding glutamate cysteine ligase, catalytic subunit (GCLC) and glyceraldehyde-3-phosphate dehydrogenase (GAPDH) (Fig. 3f). HO-1 is an important cytoprotective enzyme whose expression is achieved primarily through the modulation of its mRNA levels, and the induction of *HO-1* mRNA is a key cellular response to reactive oxygen species and other cellular stresses[8,9]. Because *HO-1* is a direct target of Star-PAP, it was selected for use in exploring the mechanism by which Star-PAP controls the expression of its select target mRNA.

We tested the hypothesis that Star-PAP and PIPKIα are necessary for *HO-1* mRNA expression during an antioxidant response. RNAi knockdown of both Star-PAP and PIPKIα decreased basal levels of *HO-1* mRNA and inhibited the maximal expression of *HO-1* mRNA in response to treatment with 100 μM t-butylhydroquinone (tBHQ)[8]

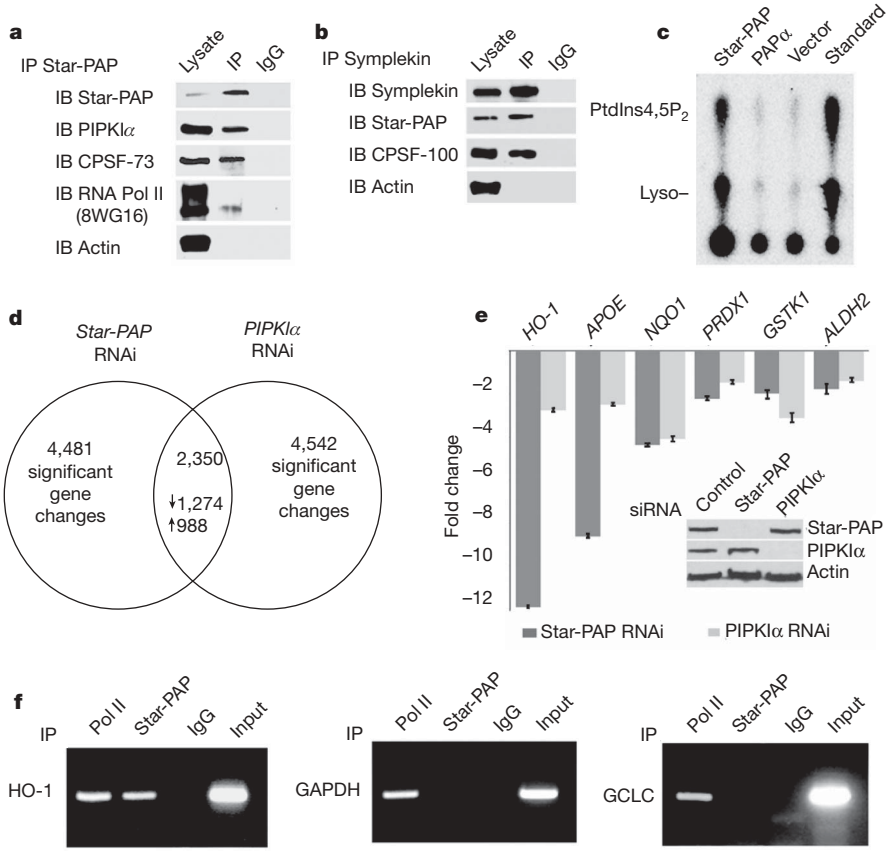

Figure 3 | Star-PAP-interacting proteins and identification of Star-PAP target mRNAs. **a**, Immunoprecipitation (IP) of Star-PAP from HEK-293 cells, followed by western blot analysis (IB) for PIPKIα, CPSF-73 and RNA Pol II (8WG16). **b**, Immunoprecipitation of symplekin from HEK-293 cells followed by western blot analysis for Star-PAP and CPSF-100. **c**, PIP kinase activity of purified PAP complexes using PtdIns4P as substrate. Lyso, PtdIns4,5P_2 degradation product in which the inositol headgroup is lacking one acyl chain. **d**, Venn diagram depicting mRNA expression profiles on *Star-PAP* or *PIPKIα* RNAi knockdown versus control. **e**, qRT–PCR analysis of selected mRNAs from **d** ($n = 3$). Error bars represent s.e.m. **f**, RNA immunoprecipitation of Star-PAP and RNA Pol II (N-20) from HEK-293 cells. Primers are listed in Supplementary Information.

(Fig. 4a). This indicated that Star-PAP and PIPKIα were required for basal and maximal expression, demonstrating that they regulate *HO-1* mRNA levels on induction of oxidative stress.

To demonstrate Star-PAP involvement in the processing and expression of *HO-1* mRNA, Star-PAP and PIPKIα were knocked down by means of RNAi, and the 3′-end formation of *HO-1* mRNA was directly examined in an *in vivo* functional assay. Star-PAP knockdown resulted in a ~20 fold increase in the quantity of uncleaved *HO-1* mRNA relative to total (Fig. 4b, c, e). In contrast, the amount of uncleaved *GCLC* mRNA was not changed by either Star-PAP or PIPKIα knockdown (Fig. 4d, f). This is consistent with reports that PAP is required for efficient 3′ cleavage by the endonuclease CPSF-73 *in vitro*[22,26,27], and indicates that Star-PAP is functioning as a PAP for the maturation of *HO-1* mRNA. PIPKIα knockdown had a smaller affect on *HO-1* mRNA cleavage (Fig. 4b, c, e), consistent with PIPKIα modifying Star-PAP function. The accumulation of unprocessed *HO-1* mRNA on Star-PAP knockdown is consistent with Star-PAP functioning as PAP *in vivo* and demonstrates that Star-PAP is required for efficient 3′-end formation of *HO-1* mRNA.

To explore the mechanism by which Star-PAP acts in the 3′ processing of mRNA, we examined the effect of stimulation of cells by tBHQ on Star-PAP complex assembly. The association of endogenous Star-PAP with PIPKIα, CPSF-73 and RNA Pol II was greatly enhanced by treatment with 100 μM tBHQ for 4 h (Fig. 4g, h). Further, Star-PAP complex purified from stably expressing cells treated with tBHQ showed a more than 15-fold increase in enzymatic activity over Star-PAP from control cells (Fig. 4i). Neither polymerase-inactive Star-PAP nor PAPα showed any increase in activity when isolated from tBHQ-treated cells (Fig. 4i, k). Treatment of cells with tBHQ caused a large increase in Star-PAP complex activity for the initiation of polyadenylation. When Star-PAP was isolated from tBHQ-treated cells, PtdIns4,5P_2 robustly stimulated Star-PAP processivity, increasing the length of the poly(A) tail, as can be seen over a time course (Fig. 4i, j). This demonstrates that tBHQ-induced signalling and PtdIns4,5P_2 modulate Star-PAP activity in two distinct yet complementary manners. These data suggest a model in which an antioxidant response induces the assembly of the Star-PAP complex, leading to a rapid initiation of 3′-end formation and polyadenylation by the Star-PAP complex. PtdIns4,5P_2 produced by PIPKIα in the complex then controls the processivity of Star-PAP, resulting in a lengthened poly(A) tail. In this manner Star-PAP may respond to oxidative stress signals, and potentially other signals, to efficiently regulate the 3′-end formation and expression of its target mRNAs.

Here we have identified and characterized a non-canonical phosphoinositide-sensitive poly(A) polymerase, Star-PAP. PtdIns4,5P_2 regulates Star-PAP processivity and thus controls the 3′-end formation

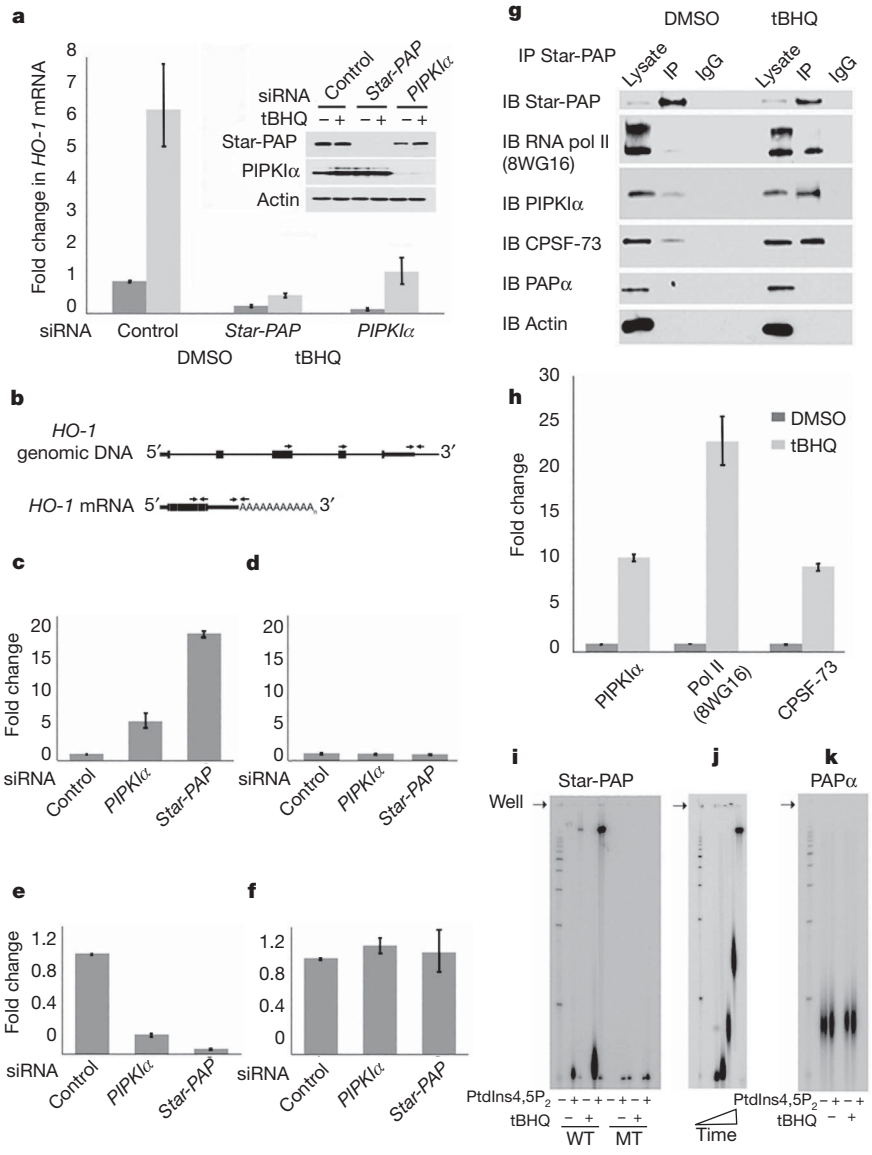

Figure 4 | Star-PAP and PIPKIα are required for efficient 3′ processing of *HO-1* mRNA by a mechanism that assembles a Star-PAP complex. **a**, qRT–PCR analysis of *HO-1* mRNA levels from HEK-293 cells transfected with *Star-PAP*, *PIPKIα* or control siRNA oligonucleotides and treated with 100 μM tBHQ ($n = 3$). DMSO, dimethylsulphoxide, vehicle control. **b**, Schematic diagram of primer set positioning used in *HO-1* mRNA cleavage analysis. **c**, **d**, Levels of uncleaved *HO-1* (**c**) and *GCLC* (**d**) mRNAs from HEK-293 cells transfected with control, *Star-PAP* or *PIPKIα* siRNA oligonucleotides. **e**, **f**, Results from **c** and **d**, respectively, normalized to total mRNA levels ($n = 3$). **g**, Immunoprecipitation (IP) of Star-PAP and detection of associated proteins from HEK-293 cells after treatment with 100 μM tBHQ. IB, immunoblot. **h**, Quantification of Star-PAP complex assembly from **g** ($n = 3$). **i**, PAP assay with affinity-purified Flag–Star-PAP (WT) or Flag–Star-PAP mutant (MT) from stably expressing HEK-293 cells subsequent to treatment with tBHQ and/or PtdIns4,5P_2. **j**, Time course subsequent to treatment with tBHQ in **i**, in the presence of PtdIns4,5P_2. **k**, Flag–PAPα activity after treatment with 100 μM tBHQ and/or the presence of PtdIns4,5P_2. All error bars represent s.e.m.

of its target mRNAs, revealing a unique function for nuclear phosphoinositides in the regulation of mRNA 3′ processing. The requirements for both Star-PAP and PIPKIα in the expression of *HO-1* mRNA provide a mechanistic link between a nuclear phosphoinositide signal transduction pathway and gene expression. Star-PAP is the first reported example of any non-canonical PAP, poly(U) polymerase (PUP)[16,28,29] or TUTase that is responsive towards phosphoinositides and assembles with the transcriptional and 3′-end-formation machinery in a signal-dependent fashion. Our model proposes (Supplementary Fig. 1) that not all nuclear pre-mRNAs require processing by PAPα. Instead, the identity and activity of the integrated PAP, PUP or TUTase varies between mRNAs in response to signalling cascades to regulate both mRNA stability and expression.

METHODS SUMMARY

Yeast two-hybrid screen. The yeast two-hybrid screen was performed by The Molecular Interaction Facility at the University of Wisconsin at Madison. Libraries screened were mouse embryonic, mouse B cell, human breast, human prostate, human placenta and mouse brain.

***In vitro* poly(A) polymerase assay.** PAP assays were performed as reported with RNA primers[13] and [α-^{32}P]ATP. An A_{15} RNA oligonucleotide was used as a substrate for the dose-dependent response of Star-PAP activity; for all other polyadenylation assays either L1 (ref. 11) or a 45-mer of the sequence $(UAGGGA)_5A_{15}$ designed to interact specifically with the Star-PAP RNA recognition motif [30] was used. The RNA product was extracted, precipitated with ethanol and dissolved in 2 × urea sample buffer and separated by PAGE in the presence of 6% urea. For the PIPn stimulation assay, the purified His-tagged Star-PAP was incubated for 10 min with PIPn micelles (Echelon Biosciences) on ice. Products were detected by a Storm 840 phosphorimager (Molecular Dynamics) and incorporation was quantified with NIH ImageJ software.

qRT–PCR and analysis of *HO-1* mRNA cleavage. Total RNA was purified from HEK-293 cells transfected with Star-PAP or PIPKIα-specific or control siRNA oligonucleotides with the RNeasy mini kit (Qiagen). For measurements of mRNA expression, RNA was reverse-transcribed with poly$(dT)_{20}$ primers and SuperScript III reverse transcriptase (Invitrogen). For assessment of mRNA cleavage, total RNA was treated with DNase I (Invitrogen) and then re-purified on RNeasy columns (Qiagen) before reverse transcription with random hexamer primers. The resulting complementary DNAs were used for qRT–PCR analysis with SYBR green detection chemistry on an ABI Prism 7000 sequence detection system (Applied Biosystems Inc.). Target mRNA levels were normalized to *GAPDH* levels. For measurement of mRNA, primers were designed to span intronic sequences to remove the possibility of DNA contamination. When this was not possible, RNA samples were treated with DNase I before RT–PCR.

Full Methods and any associated references are available in the online version of the paper at www.nature.com/nature.

Received 29 October 2007; accepted 4 January 2008.

1. Heck, J. N. *et al.* A conspicuous connection: structure defines function for the phosphatidylinositol-phosphate kinase family. *Crit. Rev. Biochem. Mol. Biol.* **42,** 15–39 (2007).
2. Gonzales, M. L. & Anderson, R. A. Nuclear phosphoinositide kinases and inositol phospholipids. *J. Cell. Biochem.* **97,** 252–260 (2006).
3. Boronenkov, I. V., Loijens, J. C., Umeda, M. & Anderson, R. A. Phosphoinositide signaling pathways in nuclei are associated with nuclear speckles containing pre-mRNA processing factors. *Mol. Biol. Cell* **9,** 3547–3560 (1998).
4. Zhao, K. *et al.* Rapid and phosphoinositol-dependent binding of the SWI/SNF-like BAF complex to chromatin after T lymphocyte receptor signaling. *Cell* **95,** 625–636 (1998).
5. York, J. D., Odom, A. R., Murphy, R., Ives, E. B. & Wente, S. R. A phospholipase C-dependent inositol polyphosphate kinase pathway required for efficient messenger RNA export. *Science* **285,** 96–100 (1999).
6. Osborne, S. L., Thomas, C. L., Gschmeissner, S. & Schiavo, G. Nuclear PtdIns(4,5)P_2 assembles in a mitotically regulated particle involved in pre-mRNA splicing. *J. Cell Sci.* **114,** 2501–2511 (2001).
7. Doughman, R. L., Firestone, A. J. & Anderson, R. A. Phosphatidylinositol phosphate kinases put PI4,5P_2 in its place. *J. Membr. Biol.* **194,** 77–89 (2003).
8. Keum, Y. S. *et al.* Induction of heme oxygenase-1 (HO-1) and NAD[P]H: quinone oxidoreductase 1 (NQO1) by a phenolic antioxidant, butylated hydroxyanisole (BHA) and its metabolite, tert-butylhydroquinone (tBHQ) in primary-cultured human and rat hepatocytes. *Pharm. Res.* **23,** 2586–2594 (2006).
9. Duckers, H. J. *et al.* Heme oxygenase-1 protects against vascular constriction and proliferation. *Nature Med.* **7,** 693–698 (2001).
10. Raabe, T., Bollum, F. J. & Manley, J. L. Primary structure and expression of bovine poly(A) polymerase. *Nature* **353,** 229–234 (1991).
11. Rouhana, L. *et al.* Vertebrate GLD2 poly(A) polymerases in the germline and the brain. *RNA* **11,** 1117–1130 (2005).
12. Cocco, L., Manzoli, L., Barnabei, O. & Martelli, A. M. Significance of subnuclear localization of key players of inositol lipid cycle. *Adv. Enzyme Regul.* **44,** 51–60 (2004).
13. Kyriakopoulou, C. B., Nordvarg, H. & Virtanen, A. A novel nuclear human poly(A) polymerase (PAP), PAPγ. *J. Biol. Chem.* **276,** 33504–33511 (2001).
14. Martin, G. & Keller, W. Mutational analysis of mammalian poly(A) polymerase identifies a region for primer binding and catalytic domain, homologous to the family X polymerases, and to other nucleotidyltransferases. *EMBO J.* **15,** 2593–2603 (1996).
15. Trippe, R. *et al.* Identification, cloning, and functional analysis of the human U6 snRNA-specific terminal uridylyl transferase. *RNA* **12,** 1494–1504 (2006).
16. Rissland, O. S., Mikulasova, A. & Norbury, C. J. Efficient RNA polyuridylation by noncanonical poly(A) polymerases. *Mol. Cell. Biol.* **27,** 3612–3624 (2007).
17. LaCava, J. *et al.* RNA degradation by the exosome is promoted by a nuclear polyadenylation complex. *Cell* **121,** 713–724 (2005).
18. Colgan, D. F. & Manley, J. L. Mechanism and regulation of mRNA polyadenylation. *Genes Dev.* **11,** 2755–2766 (1997).
19. Wang, L., Eckmann, C. R., Kadyk, L. C., Wickens, M. & Kimble, J. A regulatory cytoplasmic poly(A) polymerase in *Caenorhabditis elegans*. *Nature* **419,** 312–316 (2002).
20. Takagaki, Y. & Manley, J. L. Complex protein interactions within the human polyadenylation machinery identify a novel component. *Mol. Cell. Biol.* **20,** 1515–1525 (2000).
21. Hirose, Y. & Manley, J. L. RNA polymerase II and the integration of nuclear events. *Genes Dev.* **14,** 1415–1429 (2000).
22. Mandel, C. R. *et al.* Polyadenylation factor CPSF-73 is the pre-mRNA 3′-end-processing endonuclease. *Nature* **444,** 953–956 (2006).
23. Shatkin, A. J. & Manley, J. L. The ends of the affair: capping and polyadenylation. *Nature Struct. Biol.* **7,** 838–842 (2000).
24. Nagaoka, K., Suzuki, T., Kawano, T., Imakawa, K. & Sakai, S. Stability of casein mRNA is ensured by structural interactions between the 3′-untranslated region and poly(A) tail via the HuR and poly(A)-binding protein complex. *Biochim. Biophys. Acta* **1759,** 132–140 (2006).
25. Gilbert, C., Kristjuhan, A., Winkler, G. S. & Svejstrup, J. Q. Elongator interactions with nascent mRNA revealed by RNA immunoprecipitation. *Mol. Cell* **14,** 457–464 (2004).
26. Christofori, G. & Keller, W. 3′ cleavage and polyadenylation of mRNA precursors *in vitro* requires a poly(A) polymerase, a cleavage factor, and a snRNP. *Cell* **54,** 875–889 (1988).
27. Zhao, J., Hyman, L. & Moore, C. Formation of mRNA 3′ ends in eukaryotes: mechanism, regulation, and interrelationships with other steps in mRNA synthesis. *Microbiol. Mol. Biol. Rev.* **63,** 405–445 (1999).
28. Stevenson, A. L. & Norbury, C. J. The Cid1 family of non-canonical poly(A) polymerases. *Yeast* **23,** 991–1000 (2006).
29. Kwak, J. E. & Wickens, M. A family of poly(U) polymerases. *RNA* **13,** 860–867 (2007).
30. Ding, J. *et al.* Crystal structure of the two-RRM domain of hnRNP A1 (UP1) complexed with single-stranded telomeric DNA. *Genes Dev.* **13,** 1102–1115 (1999).

Supplementary Information is linked to the online version of the paper at www.nature.com/nature.

Acknowledgements We thank J. L. Manley for the gift of antibodies against CPSF-73, CstF-64 and PAPα; M. Wickens for the generous gift of the PAPα construct and for advice and discussion; D. Brow, S. Miyamoto, D. Wassarman and R. Tibbetts for reading the manuscript and for comments; and C. Song for technical assistance in the early parts of the project. R.A.A. is supported by grants from the National Institutes of Health (NIH). M.L.G., D.L.M. and C.S. were supported by the American Heart Association. C.A.B. is supported by the National Research Service Award. D.L.M. and M.L.G. received Research Training Grant support from the NIH.

Author Contributions D.L.M. contributed to Figs 1a, d, f, 2, 3a, b, 4g–k and Supplementary Figs 1, 2, 4–7. M.L.G. contributed to Figs 1a, 3c, f, 4a–f and Supplementary Fig. 1. C.A.B. contributed to Fig. 3d, e, Supplementary Fig. 1 and Supplementary Tables 1 and 2. C.S. contributed to Fig. 1a, c, e and Supplementary Figs 3 and 6. P.W. and C.K. analysed the microarray data. R.A.A. directed the experimental approach and project. D.L.M., M.L.G., C.A.B. and R.A.A. analysed and interpreted the experiments, and conceptualized and wrote the paper.

Author Information The Star-PAP sequence is deposited in the NCBI Library under accession number NP_073741. The microarray data discussed in this publication have been deposited in NCBI's Gene Expression Omnibus (GEO, http://www.ncbi.nlm.nih.gov/geo/) and are accessible through GEO series accession number GSE9361. Reprints and permissions information is available at www.nature.com/reprints. Correspondence and requests for materials should be addressed to R.A.A. (raanders@wisc.edu).

METHODS

DNA constructs. The N-terminal (residues 1–439) and C-terminal (residues 440–562) fragments of PIPKIα were amplified by PCR and cloned into the pCMV–HA mammalian expression vector (Invitrogen). The full-length PIPKIα open reading frames and the PIPKIα C terminus (residues 440–562) were subcloned into the pGEX-5X-2 *Escherichia coli* expression vector (Amersham Biosciences).

The Star-PAP open reading frame was amplified by PCR from *Homo sapiens* cDNA: FLJ22347 fis, clone HRC06188 (NCBI accession number NM_022830) was inserted into pCMV–Flag (Invitrogen) pCMV–HA, pCMV–Myc and pET28c (Novagen) expression vectors. The N terminus (residues 1–328) of Star-PAP fragment was amplified by PCR and cloned into pGEX-5X-2 (Amersham Biosciences).

Site-directed mutagenesis was performed by using PCR-primer overlap extension with mutagenic primers. Primers used were 5′-gtccatggctgtgatcttgccctcttcttggatctgggtg-3′ and 5′-cacccagatccaagaagagggcaagatcacagccatggac-3′ for Star-PAP (D218A), and 5′-gtccatggctgtgctcttgccctcttcttggatctgggtg-3′ and 5′-cacccagatccaagaagagggcaagagcacagccatggac-3′ for Star-PAP (D216A/D218A).

PAPα was subcloned into pCMV–Flag mammalian expression vector (Invitrogen) for Flag complex purification.

Expression and purification of recombinant proteins from *E. coli*. Epitope-tagged proteins were expressed in *E. coli* strain BL-21 and purified with Ni-nitrilotriacetate-agarose (Qiagen) or glutathione-Sepharose (GE Healthcare) in accordance with the manufacturer's instructions. The eluates were dialysed, flash frozen and stored at −80 °C.

Antibodies. Polyclonal Star-PAP antiserum was generated by Covance from rabbits boosted with purified GST-tagged N terminus (residues 1–328) as the antigen and affinity purified over a column coupled with His-tagged Star-PAP N terminus (residues 1–328), or by using purified full-length GST–Star-PAP as antigen and affinity purified from precleared serum over a column coupled with GST–Star-PAP. The following antibodies were used: anti-HA and anti-Myc (Covance), anti-Flag M5 (Sigma), anti-SM (Y12) (Stratech) anti-SC-35 (BD Pharmingen), anti-symplekin (BD Transduction Laboratories), anti-CPSF-100 and RNA Pol II (N-20) (Santa Cruz Biotechnology), anti-RNA polymerase II antibody 8WG16 (Neoclone), and anti-β-actin ascites (MP Biomedicals). PIPKIα and PIPKIγ polyclonal antibodies were generated and used as reported previously[6]. Anti-PAPα was also purchased from Bethyl Labs. All secondary antibodies were from Jackson Immunoresearch Laboratories.

Oligo(dT)/RNase H digestion. For oligo(dT)/RNase H digestion, PAP reactions were performed with a [γ-^{32}P]ATP 5′-labelled L1 RNA primer at 4 μM and 1 mM unlabelled NTPs. Digestion of poly(A)$^+$ RNA was performed in 200 mM KCl, 1 mM EDTA, 20 mM Tris-HCl pH 8.0, 30 mM $MgCl_2$ and 20 U RNasin. Oligo(dT) (8 μM) was used for annealing to the RNA primer, and digestion was performed at 37 °C for 90 min with 4 U of RNase H (Promega).

***In vitro* terminal uridylyl transferase and nucleotide competition assays.** TUTase assays were performed as reported[15] with recombinant His–Star-PAP expressed and purified from *E. coli* BL-21. Total cellular RNA was purified from HeLa cells with the miRNeasy mini kit (Qiagen), and the L1 substrate was commercially synthesized (Integrated DNA Technologies). Nucleotide competition assays were performed under both PAP and TUTase conditions, with titration of up to fivefold excess unlabelled nucleotide triphosphate.

Cell culture, transfection, and immunofluorescence microscopy. HeLa and HEK-293 cells were cultured in DMEM medium (Mediatech, Inc.) supplemented with 10% fetal bovine serum (Invitrogen) and antibiotics. tBHQ (Sigma) was dissolved in dimethylsulphoxide and used at final concentration of 100 μM. HEK-293 and HeLa cells were transfected using the calcium phosphate method except for siRNA oligos, which were transfected into HeLa cells using Oligofectamine transfection reagent (Invitrogen). siRNA oligonucleotides used were as follows: Star-PAP-1, 5′-AACUACGAGCTGCGAGAAA-3′; Star-PAP-2, 5′-GUGUGUUUGUCAGUGGCUU-3′; PIPKIα-1, 5′-GGUGCCAUCCAGUUAGGCA-3′; PIPKIα-3, 5′-GAAGUUGGAGCACUCUUGG-3′; control, 5′-AGGUAGUGUAAUCGCCUUG-3′. Immunofluorescence microscopy was performed as described[6].

Immunoprecipitations. HeLa and HEK-293 cells were lysed in IP buffer (100 mM KCl, 50 mM Tris-HCl pH 7.4, 5 mM EDTA, 0.5% Nonidet P40, 100 μg ml^{-1} RNase A, 200 mM $NaVO_4$, 50 mM L-glycerophosphate, 50 mM NaF and 1 × EDTA-free protease inhibitor cocktail (Roche) with gentle sonication (power = 11%, five times for 3 s). Lysates were centrifuged at 40,000*g* and the supernatant was incubated at 4 °C for 4 h with 4 μg of the indicated antibody or control IgG, followed by incubation at 4 °C for 1 h or overnight with Protein A-Sepharose. Beads were washed extensively and resuspended in 1 × SDS–PAGE loading buffer for western blot analysis.

Affinity purification of Flag-fusion proteins: PtdInsP kinase and PAP assay. Flag-fusion proteins were affinity purified with anti-Flag (M2) affinity gel (Sigma-Aldrich) from HEK-293 cells stably expressing Flag–Star-PAP, in accordance with the manufacturer's instructions. PtdInsP kinase activity was measured as previously reported[31]. PAP activity was measured as described[13] with 1 mM ATP and 10 μCi of [α-^{32}P]ATP, Tris-HCl pH 7.9, 2.5 mM $MgCl_2$, 50 μM PtdIns4,5P_2 at 37 °C for 60 min with the 45-mer RNA oligonucleotide $(UAGGGA)_5A_{15}$ as an RNA substrate.

Northern blotting. A DNA probe representing base pairs 541–1046 of human Star-PAP was generated with the Strip-EZ PCR kit (Ambion) and used to probe the human multiple-tissue northern blot II membrane (Ambion) in accordance with the manufacturer's instructions. The blots were revealed with a Storm 840 phosphorimager (Molecular Dynamics).

Microarray analysis. Total RNA was extracted from HEK-293 cells transfected with Star-PAP-specific or PIPKIα-specific or control siRNA oligonucleotides with the RNeasy mini isolation kit (Qiagen) ($n = 3$). Labelled probes for microarray hybridization were generated with MessageAmp II-Biotin Enhanced kit (Ambion) in accordance with the manufacturer's instructions. U133A plus 2.0 arrays (Affymetrix) were used for expression profiling. Labelling, hybridization, washing, scanning and analysis of gene chips were performed at the University of Wisconsin Gene Expression Center. The data from the control siRNA treatment were used as a baseline expression for comparison with the *Star-PAP* and *PIPKIα* siRNA-treated samples.

Statistical analysis of microarray data. The measurement of changes in expression was analysed statistically with the empirical Bayes methodology EBarrays, which is implemented in R, a publicly available statistical analysis environment (http://www.r-project.org). Posterior probabilities of differential expression (DE) were calculated assuming the log-normal normal (LNN) expression model. The threshold was determined with a direct posterior probability approach[32], which seeks to control the conditional false discovery rate (cFDR) at a specific level.

Of the more than 47,000 transcripts and variants, the LNN model identified 6,311 DE genes with threshold 0.888 to control cFDR at 0.01 for the *Star-PAP* knockdown and 6,213 DE genes with threshold 0.878 to control cFDR at 0.01 for the *PIPKIα* knockdown. The fold changes in the intensity signals were calculated in Microsoft Excel from the following formula: fold change = −[(average signal intensity in control group)/(average signal intensity in knockdown group)] or fold change = [(average signal intensity in knockdown)/(average signal intensity in control group)]. The probe ID, gene ID, fold change, gene name and gene ontology are summarized in Supplementary Tables 1 and 2.

RNA immunoprecipitation. RNA immunoprecipitations were performed as reported[25], with antibodies against Star-PAP and RNA Pol II (clone N-20). A total of 10^7 HEK-293 cells were used per immunoprecipitation condition. RNA was purified from the immunoprecipitates with TRI reagent (Sigma) in accordance with the manufacturer's instructions. RNA was analysed by RT–PCR with the One Step RT–PCR kit (Qiagen) and gene-specific primers listed below.

Primers for real-time PCR analysis of mRNA levels. ALDH2 fw, 5′-ACCTTCGTGCAGGAGGACAT-3′; ALDH2 rv, 5′-CGTGTTGATGTAGCCGAGGA-3′; APOE fw, 5′-CGTTGCTGGTCACATTCCTG-3′; APOE rv, 5′-CCTGCACCTGCTCAGACAGT-3′; GAPDH fw, 5′-GAAGGTCGGAGTCAACGGATTT-3′; GAPDH rv, 5′-GAATTTGCCATGGGTGGAAT-3′; GCLC fw, 5′-AAGTTCTTGAAACTCTGCAAGAGAAGG-3′; GCLC rv, 5′-GCCTCAACTGTATTGAACTCGGAC-3′; GSTκ1 fw, 5′-AAACAAGCCTCCAGGTCTGC-3′; GSTκ1 rv, 5′-GGACGCTTTCTCCAGCATCT-3′; HO-1 fw, 5′-CCACCAAGTTCAAGCAGCTCTA-3′; HO-1 rv, 5′-GCTCCTGCAACTCCTCAAAGAG-3′; NQO1 fw, 5′-GAACTTCAATCCCATCATTTCCAG-3 NQO1 rv, 5′-CAGCTTCTTTTGTTCAGCCACAAT-3 PRDX1 fw, 5′-TGCCAAGTGATTGGTGCTTC-3′; PRDX1 rv, 5′-AAAAGGCCCCTGAACGAGAT-3′.

Primers for cleavage analysis. HO-1 Clv fw, 5′-GGCACTGTGGCCTTGGTCTAA-3′; HO-1 Clv rv, 5′-TCCTACCGAGCACGCAAGAA-3′; GCLC Clv fw, 5′-ATGCCTGGTTTTCGTTTGCA-3′; GCLC Clv rv, 5′-AGCTGTGGAACTCACACACACTCA-3′.

31. Ling, K., Doughman, R. L., Firestone, A. J., Bunce, M. W. & Anderson, R. A. Type Iγ phosphatidylinositol phosphate kinase targets and regulates focal adhesions. *Nature* **420**, 89–93 (2002).
32. Kendziorski, C. M., Newton, M. A., Lan, H. & Gould, M. N. On parametric empirical Bayes methods for comparing multiple groups using replicated gene expression profiles. *Stat. Med.* **22**, 3899–3914 (2003).